



## ORIGINAL ARTICLE

# The assessment of apoptosis, toxicity effects and anti-leishmanial study of Chitosan/CdO core-shell nanoparticles, eco-friendly synthesis and evaluation



Sina Bahraminegad<sup>a</sup>, Abbas Pardakhty<sup>b</sup>, Iraj Sharifi<sup>a</sup>, Mehdi Ranjbar<sup>b,c,\*</sup>

<sup>a</sup> Leishmaniasis Research Center, Kerman University of Medical Sciences, Kerman, Iran

<sup>b</sup> Pharmaceutics Research Center, Institute of Neuropharmacology, Kerman University of Medical Sciences, Kerman, Iran

<sup>c</sup> Neuroscience Research Center, Institute of Neuropharmacology, Kerman University of Medical Sciences, Kerman, Iran

Received 3 January 2021; accepted 10 February 2021

Available online 22 February 2021

## KEYWORDS

Core shell nanostructures;  
Nanoparticles;  
Anti leishmanial effects;  
*Leishmania major*

**Abstract** Leishmaniasis is a parasitic disease that can be transmitted to individuals by a species of the *Leishmania* flagellated protozoan. Due to problems such as toxicity, high cost, long duration of treatment, increased drug resistance, painful injections, and side effects, leishmaniasis is considered as an important epidemic in people with systemic deficits. Therefore, in this study, new core-shell nanostructures were introduced as anti-leishmanial drugs for the first time. The expression of *IFN-γ*, *TNF-α*, *IL-4*, and *IL-12* genes were evaluated by real-time PCR. Investigations revealed that CdO/Chitosan core shell nanostructures decreased the proliferation of promastigotes ( $p < 0.0001$ ). The number of promastigotes were reduced in the presence of different concentrations of the nanostructures. The average value of  $IC_{50}$  for promastigotes was about 0.6  $\mu\text{g/mL}$ . The concentration of the drug that prevented the growth of 50% of macrophages for core shell nanostructures was 1.256  $\mu\text{g/mL}$ . The level of apoptosis in *leishmania* promastigotes in the presence of nanodots at the concentrations of 1, 0.5, and 0.25  $\mu\text{g/mL}$  was 56%, 31%, and 23%, respectively. Furthermore, according to the results, it can be concluded that the level of gene expression pertaining to Th1 was significantly up-regulated ( $p < 0.001$ ). This study showed that the core-shell nanodots of chitosan/cadmium oxide inhibit the proliferation of promastigotes and increase the apoptosis of *leishmania* promastigotes.

© 2021 The Authors. Published by Elsevier B.V. on behalf of King Saud University. This is an open access article under the CC BY-NC-ND license (<http://creativecommons.org/licenses/by-nc-nd/4.0/>).

## 1. Introduction

Nowadays, despite the many advances that have been made in medicine and especially in the control of infectious diseases, some of these diseases are still considered as health concerns. Leishmaniasis, which is classified as a parasitic disease, has been observed around the world (Casa et al., 2018; Fanti

\* Corresponding author.

E-mail address: [Mehdi.Ranjbar@kmu.ac.ir](mailto:Mehdi.Ranjbar@kmu.ac.ir) (M. Ranjbar).

Peer review under responsibility of King Saud University.



Production and hosting by Elsevier

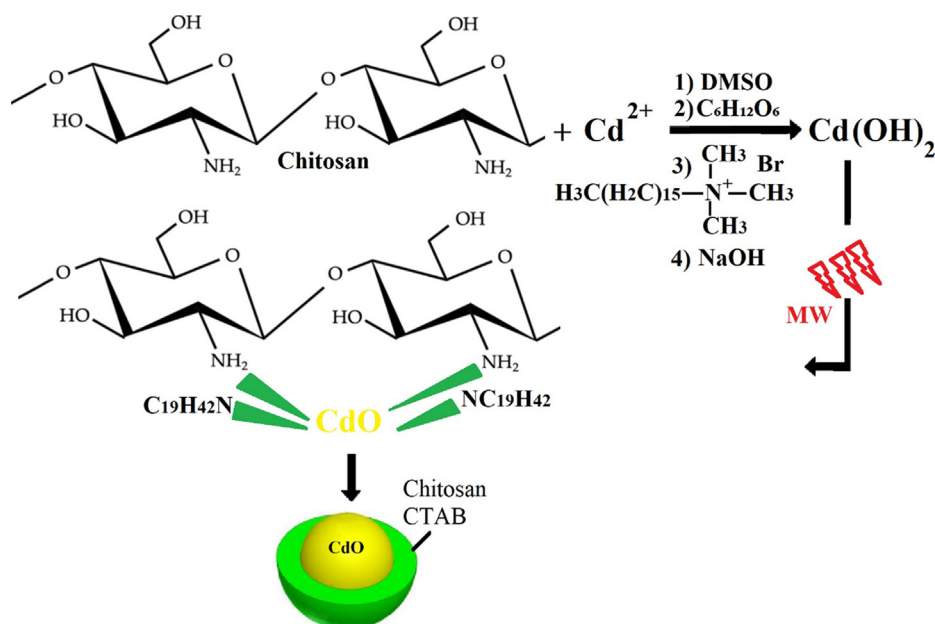
et al., 2018; Ghorbani and Farhoudi, 2018). The World Health Organization (WHO) has included this disease in the list of six important diseases in tropical and subtropical regions due to its health importance (Edrisiyan, 1996; Kubba et al., 1987). Leishmaniasis is a common disease of humans and animals which occurs in three forms, cutaneous, visceral (kala-azar), and cutaneous-mucosal leishmaniasis. The most common cutaneous forms are the dry or urban (zoonotic cutaneous leishmaniasis) and wet or rural (anthroponotic cutaneous leishmaniasis) forms, which are caused by *L. tropica* and *L. major*, respectively (Zink et al., 2006; Moemenbellah-Fard, 2003). The disease is widespread in all continents except Australia. According to WHO, 12 million people worldwide are infected with various types of leishmaniasis, and a population of about 350 million people are at risk for the disease (Alrajhi, 2003; Khanjani et al., 2018; Kassiri et al., 2014). A number of drugs such as antimonial pentavalent antimoniate, sodium stibogluconate, pentamidine, and amphotericin B are used in the first-line systemic treatment of leishmaniasis (Carvalho et al., 2019; Croft and Olliaro, 2011; Tiuman et al., 2011). Problems such as inaccessibility of these drugs, high toxicity, side effects, and drug resistance are the important concerns in a leishmaniasis epidemic (Belani et al., 2012). Chitosan nanoparticles (NPs) enhance resistance to microbial infections due to their antioxidant activity and immune-stimulating properties (Akbari et al., 2017). Metal-based NPs are known for their small size and high surface area (Aderibigbe, 2017). Today, green synthesis of nanoparticles is one of the most effective and least expensive methods of making nanoparticles in various fields of application (Parveen et al., 2016; Hussain et al., 2016; Raveendran et al., 2003). These particles exert their antimicrobial activity by producing reactive oxygen species (ROS) that cause microbial damage. The ability of these particles to bind to DNA or RNA also inhibits microbial replication processes (Arvizo et al., 2012; Zain et al., 2014). Core-shell NPs are composed of two or more different compounds (metal and metal oxide, polymer, element, or biomolecule); one of these compounds acts as the nucleus and is located at

the center of the particle and the other compound or compounds are located around the nucleus and play the role of the shell (López-Lorente et al., 2011). A wide range of organic and inorganic compounds such as polymers (Ng et al., 2013), biomolecules, silica, and metallic as well as non-metallic compounds can be placed on the surface of these NPs. The advantage of covering NPs with different compounds can be more than just protecting the core (Cortie and McDonagh, 2011; Zhao et al., 2008). Stability, biocompatibility, selective function, targeted transfer, and identification of biological compounds, such as cells (Ong et al., 2017), proteins, nucleic acids (Shen et al., 2014), enzymes (Tan et al., 2013), microbes, etc., are some of the reasons that different compounds are placed on the surface of these particles (Khatami et al., 2018). Nanoparticle such as Ag NPs (Ma and Yang, 2016), CuO NPs (Gopinath et al., 2016) and ZnO nanostructures (Premanathan et al., 2011) plays important and influential role on the apoptosis, toxicity effects. To our knowledge, based on a review of scientific sources, there is no report on using core-shell nanostructures that are electrostatically conjugated to the CdO NPs for an anti-leishmanial study. In the present investigation, apoptosis of *Leishmania major* was assessed at different concentrations of CdO/chitosan core-shell nanostructures with a control drug and amphotericin B. CdO/chitosan core-shell nanostructures were characterized with dynamic light scattering (DLS), scanning electron microscopy (SEM), transmission electron microscopy (TEM), energy dispersive X-ray analysis (EDX), X-ray powder diffraction (XRD), Fourier-transform infrared spectroscopy (FT-IR), and thermogravimetry analysis (TGA).

## 2. Materials and methods

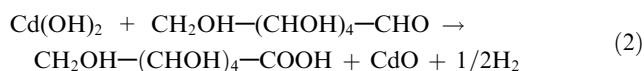
### 2.1. Preparation of CdO/chitosan NPs

To prepare the CdO/chitosan NPs, at the first, 0.05 g of Cd ( $(\text{NO}_3)_2 \cdot 4\text{H}_2\text{O}$ ) was dissolved in double-distilled water and



**Scheme 1** The mechanism of the formation process of the CdO/Chitosan core shell nanostructures.

dimethyl sulfoxide with a ratio of 2:1 under a reflux system at 50 °C for 30 min and stirred at a speed of 400 rpm using a magnetic stirrer. Then 0.001 g of  $C_6H_{12}O_6$ , as green reductant and capping agent, as well as 5 mL of sodium hydroxide 2 M, to adjust the pH in the reaction medium, were added to the solution for 30 min at 50 °C and 400 rpm. Then, after adding 5 mg of sodium dodecyl sulfate (CTAB) to stabilize the electrostatic atmosphere of the ions, 2 mL of NaOH was added dropwise to the reaction medium for 30 min. Then the mixture was placed in a microwave oven at a power of 300 W for 10 min. In the next step, 0.05 g of chitosan powder was added to double-distilled water and ethanol with a ratio of 1:4. The solution was stirred for 30 min on a heater at 50 °C using a magnetic stirrer. Then 0.03 g of CdO NPs from the first step was added to the mixture from the previous step drop by drop for 30 min at 50 °C with the help of a magnetic stirrer. After that, the reaction mixture was heated for 30 min in a reflux system. Finally, the resulting mixtures were placed in a microwave at 100 W for 10 min. We predict that the formation process of the CdO/Chitosan core shell nanostructures can be according to Scheme 1. In this study  $C_6H_{12}O_6$  was used as the green reductant, according to the relation of the following equation (Engelbrekt et al., 2009; Tabrizi and Varkani, 2014; Liu et al., 2006):



## 2.2. Preparation of *Leishmania major* parasites and macrophage cells

*Leishmania major* promastigotes were cultured in a 25-mL flask containing RPMI-1640 medium, 10% fetal bovine serum (FBS), and the antibiotics penicillin and gentamicin at 24 °C. Macrophages were obtained from the Pasteur Institute of IRAN. The macrophages were placed in a flask in an incubator at 37 °C with 5%  $CO_2$ . The flask was removed from the incubator daily and after observation under an inverted microscope, under sterile conditions, the supernatant of the cells was removed and fresh RPMI-1640 medium plus 10% or 50% FBS was added to the flask.

**Table 1** The specific primers and reference genes sequences.

Template	Forward and reverse sequences (5'-3')
Ifn- $\gamma$	F-ACAGCAAGGCGAAAAAGGATG R-TGGTGGACCACTCGGATGA
IL-12	F-CTGTGCCTTGGTAGCATCTATG R-GCAGAGTCTCGCCATTATGATTC
Tnf- $\alpha$	F-CAGGCGGTGCCTATGTCTC R-CGATCACCCCGAAGTTCAGTAG
IL-4	F-GGTCTCAACCCCGAGCTAGT R-GCCGATGATCTCTCAAGTGAT
GApdh	F-AGGTCCGTGTGAACGGATTG R-TGTAGACCGTGTAGTTGAGGTCA

## 2.3. Evaluation of drug toxicity to macrophages

Flow cytometry was used to measure the drug toxicity. To do this,  $10^6$  macrophages were counted under a microscope and plated in a 6-well microplate and incubated at 37 °C in a  $CO_2$  incubator for 24 h. After the incubation, 100  $\mu$ L of different dilutions of the drug were added to the macrophages and the volume was increased to 1 mL with culture medium. Then the cells were incubated again at 37 °C in a  $CO_2$  incubator for

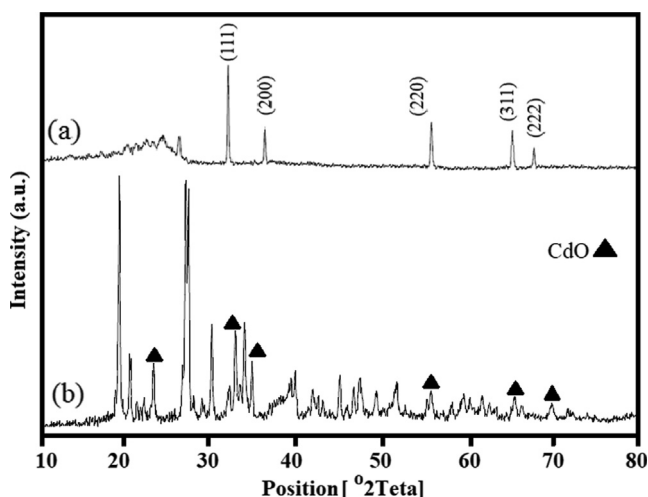


**Fig. 1** XRD analysis of the CdO nanoparticles (Foroughi et al., 2017) (a) and as-synthesized CdO/Chitosan core shell nanostructures (b).

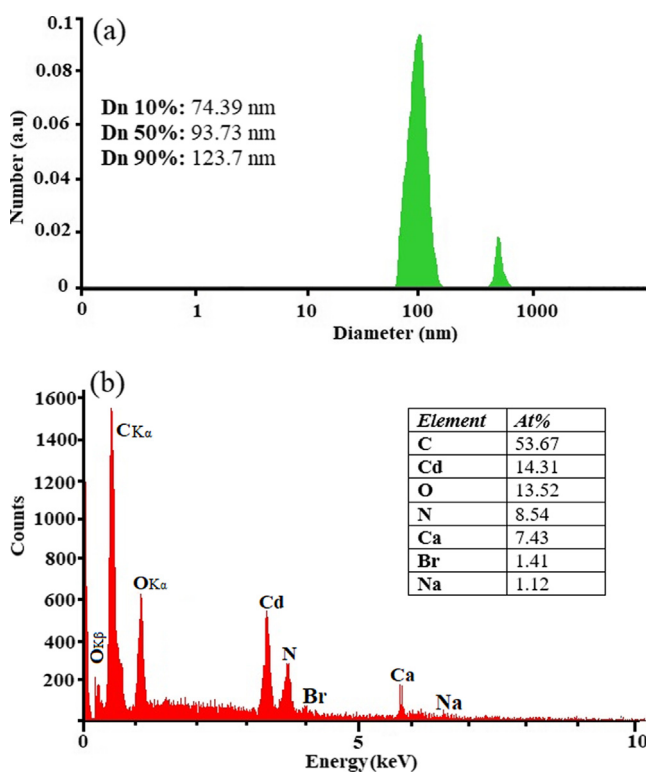


**Fig. 2** DLS data diagram (a) and EDAX analysis of as-synthesized CdO/Chitosan NPs.

72 h. After this incubation period, the cells were scrapped and transferred to 0.5-mL microtubes and centrifuged to settle the macrophages. Then they were washed twice with the PBS solution and 1 mL of binding buffer was added to them. Next, 100 mL of the whole mixture was removed and 5  $\mu$ L of annexin V-IFTC and 5  $\mu$ L of 7-aminoactinomycin D (AAD7) were added to it and the mixture was subsequently evaluated by a flow cytometer (BD FACSCalibur™, San Jose, California, USA).

#### 2.4. Assessment of parasitic apoptosis by flow cytometry

To quantify the apoptosis of parasites, the Calbiochem apoptosis diagnosis kit was used. According to the kit instructions, the parasites were stained by annexin V-IFTC and 7AAD and analyzed using a Becton Dickinson flow cytometer. To perform this assay, first, the test specimens containing about one million parasites per milliliter of total reaction volume and 100  $\mu$ L of different concentrations of amphotericin B and chitosan/cadmium oxide NPs were added to sterile microtubes. The microtubes were centrifuged at 14,000g for 15 min, and then the supernatant was discarded and the sediments in all the microtubes were washed three times with the PBS solution. The binding buffer solution was

added to the washed precipitate and kept in a dark place at 26 °C for 20 min. In the last step, antibodies were added to each microtube, mixed well, and tested using a flow cytometer (BD FACSCalibur, San Jose, California, USA).

#### 2.5. RNA isolation and analysis

In this study, RNA was extracted with the RNeasy Mini Kit (Qiagen, Chatsworth, California, USA) according to the manufacturer's instructions at various concentrations of effective drug combination and untreated control. The quality and quantity of the extracted RNA was determined by a Nanodrop spectrophotometer (ND-2000, Thermo Scientific Fisher, US) and 2% agarose gel electrophoresis, respectively. The cDNA was synthesized by the RT reagent kit (Takara, Japan) using 100 ng of the extracted RNA in a FlexCycler (Analytik Jena, Germany) at 37 °C for 15 min. Table 1 indicates the specific primers and reference gene sequences. For the normalization purposes, glyceraldehyde 3-phosphate dehydrogenase (GAPDH) was used as a reference gene and they were detected by quantitative real-time PCR (q-PCR) assay; also a no-cDNA sample was used as a negative control in each run. The qPCR reactions and treatments were run in a total volume of 15  $\mu$ L

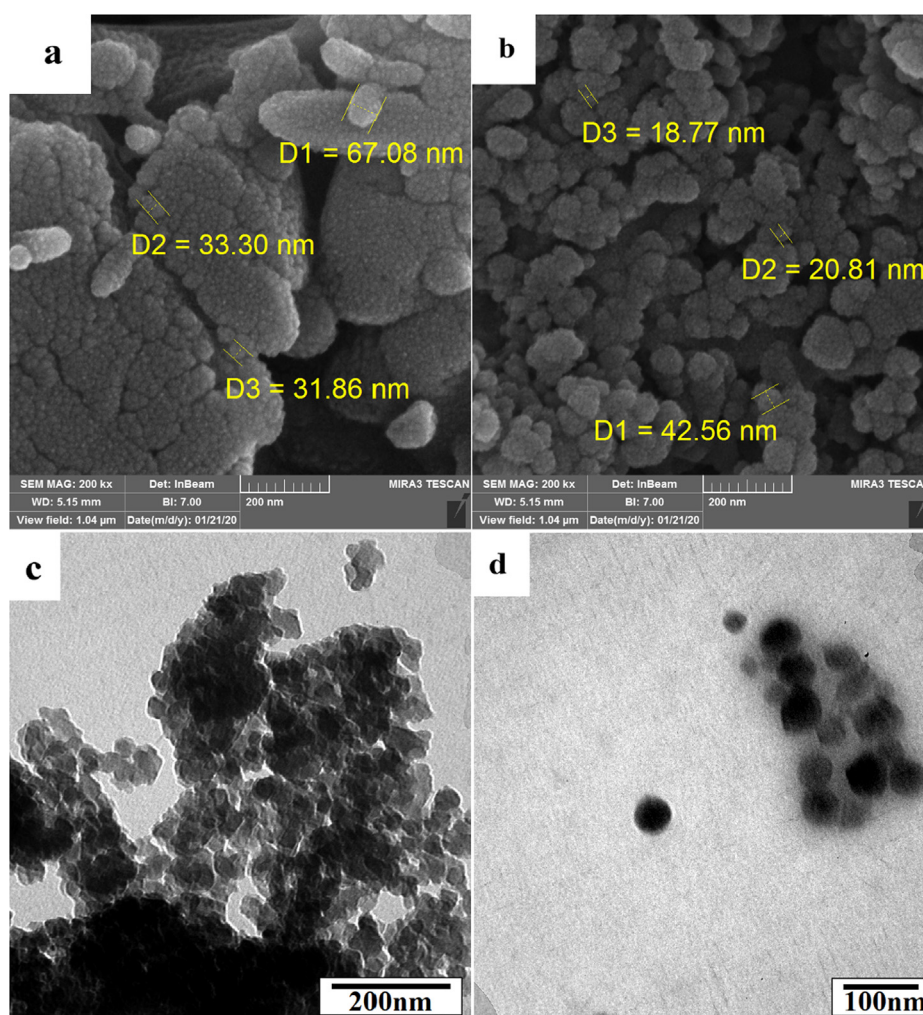


**Fig. 3** SEM images of chitosan (a), CdO/Chitosan NPs (b), TEM image of CdO/Chitosan core/shell structure with scale 200 nm (c) and with scale 100 nm.

using SYBR® Premix Ex Taq™ II (Takara, Japan) based on the recommended protocol in a qPCR system (Rotor-Gene Q, Qiagen) (Parizi et al., 2019).

### 2.6. Statistical analyses

Statistical data analyses were performed using two-way analysis of variance (ANOVA) and *t*-test in the SPSS software ver. 20 (Chicago, Illinois, USA). IC50 and CC50 were measured by probit analysis in SPSS software and the results were considered significant at  $P \leq 0.0001$ .

## 3. Results and discussion

### 3.1. Characterization of CdO/chitosan NPs

In order to investigate the crystalline properties and determine the phase of the CdO/Chitosan core shell nanostructures X-ray powder diffraction (XRD) analysis was performed. The XRD

results show that the structure formed is a combination of CdO structures and the factors such as CTAB, chitosan and glucose which are used in the preparation of the CdO/Chitosan core shell nanostructures. XRD analysis for the CdO nanoparticles (Foroughi et al., 2017) and as-synthesized CdO/Chitosan core shell nanostructures are shown in Fig. 1a and b respectively.

In this study, the DLS method was used to determine the hydrodynamic diameter. The particle size of the CdO/chitosan NP sample was analyzed by DLS under the following conditions: the wavelength of 657 nm, diffusion coefficient of  $12.35 \mu\text{m}^2/\text{s}$ , and intensity of 93.59%. To measure the particle size, 0.1 mL of the CdO/chitosan NP solution in 2 mL of deionized water (DI H<sub>2</sub>O) was poured into a polystyrene cuvette and the particle size was calculated at 25 °C. Fig. 2a shows the size distribution by the intensity of CdO/chitosan NPs in the solution. The size of the CdO/chitosan NP sample was calculated at about 120 nm. According to the DLS data analysis, Dn 10%: 74.39 nm, Dn 50%: 93.73 nm, Dn 90%: 123.7 nm were obtained. The particle size determined by the DLS detec-

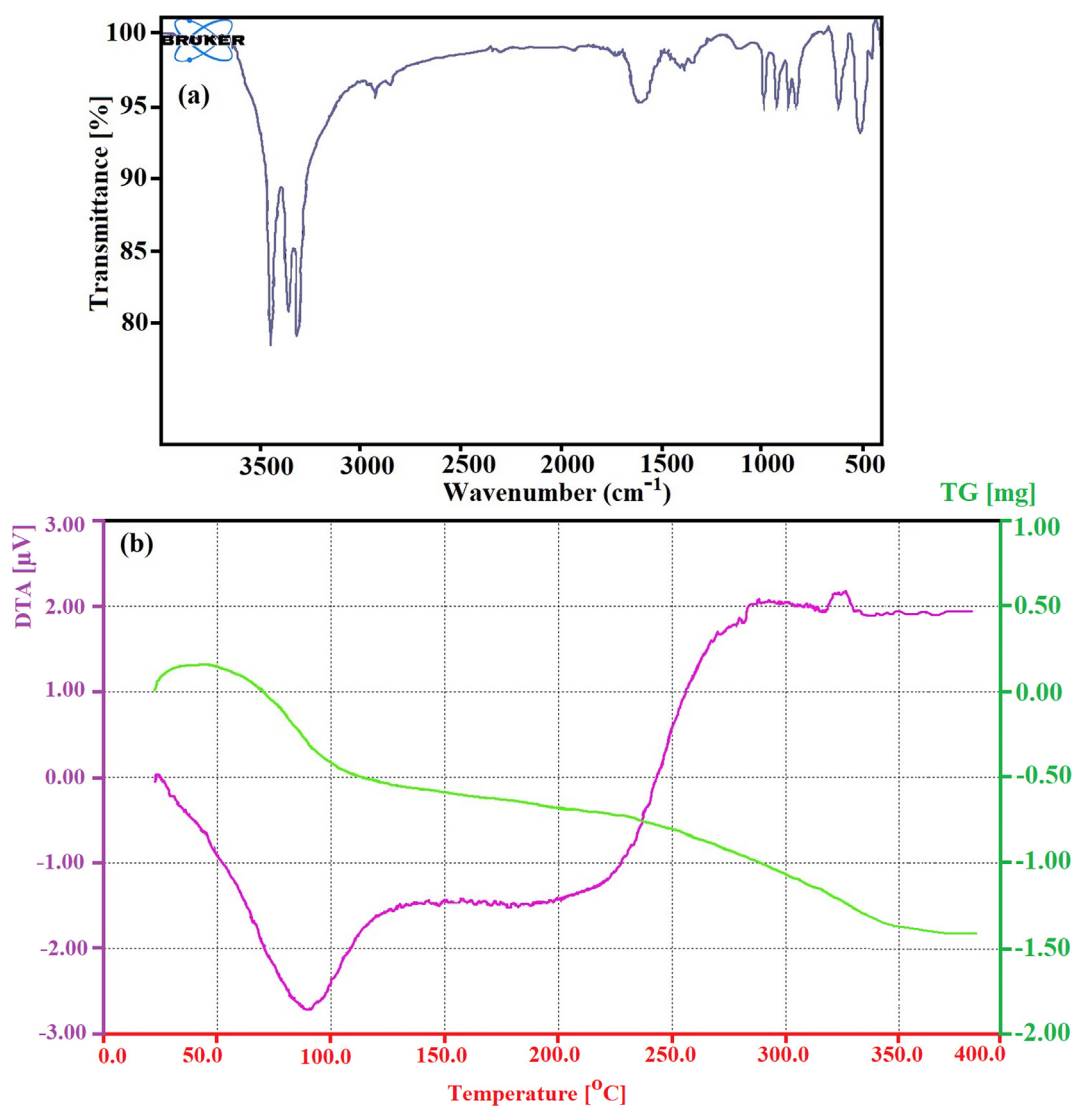


**Fig. 4** The FT-IR analysis in the range of  $500 \text{ cm}^{-1}$  up to  $3500 \text{ cm}^{-1}$  for CdO/Chitosan NPs (a) and the TGA diagram for as-synthesized the CdO/Chitosan NPs (b).

tor was slightly larger than the nominal size, probably because this method measures the hydrodynamic size rather than the physical size. To obtain the exact percentage of elements in the final products, EDX was used. EDX analysis is a non-destructive test for the CdO/chitosan NP sample, which is shown in Fig. 2b. Elements such as C, N, and O can be related to the presence of chitosan. Moreover, elements such as Br, Na, and Ca can be related to the presence of CTAB, NaOH, and distilled water, respectively.

The shape and size of the CdO/chitosan NPs were measured using SEM. The results of SEM imaging of chitosan and CdO/chitosan NPs are shown in Fig. 3a and b, respectively (with the magnification of 200 nm). As can be seen, SEM images of chitosan structures show an agglomerated zone with a uniform dispersion with a nanoparticle size of about 33 nm to 67 nm. The CdO/chitosan NP samples were shown to have quite a small size (about 18 nm to 40 nm) with uniform spherical shape. TEM was used to further investigate the particle size and shape of the structures. Fig. 3c shows the TEM image for CdO/chitosan NPs. The TEM images are in good agreement with the SEM images. Smaller-sized CdO/chitosan NPs have many positive aspects such as good conductivity, chemical stability, and catalytic and antibacterial activities, which would make these NPs suitable for many practical applications.

The FT-IR spectroscopy is a non-destructive technique that can be used not only for qualitative analysis (identification) of materials but also for quantitative analysis (measuring the amount) for characterization of the chemical composition and functional groups in the CdO/Chitosan core shell nanostructures. The FT-IR analysis peaks were measured in the range of  $500\text{ cm}^{-1}$  to  $3500\text{ cm}^{-1}$  for CdO/chitosan NPs. Fig. 4a shows narrow and sharp peaks at the area of

$3100\text{ cm}^{-1}$  up to  $3500\text{ cm}^{-1}$  which can be due to the moisture in the structure and the O—H bonds in NaOH and also N—H and H—N—H bonds related to cetyltrimethylammonium bromide (CTAB) with  $\text{H}^+$  ions free in the reaction environment (Boeckx and Maes, 2012). The peaks at the  $1652\text{ cm}^{-1}$  region belonged to the N—H functional group in the chitosan polymers. The peak at the  $2923\text{ cm}^{-1}$  region was related to the C—H bonds in the chitosan polymer. In addition, the presence of peaks in the range of  $400\text{--}700\text{ cm}^{-1}$  indicated the bonding of Cd and O elements. To investigate mass loss with time under certain temperature conditions, TGA was used under nitrogen atmosphere with a heating rate of  $10\text{ }^\circ\text{C}/\text{min}$  from  $25\text{ }^\circ\text{C}$  up to  $400\text{ }^\circ\text{C}$ . The main principle of TGA is that mass change for a sample can be studied under programmed conditions. Fig. 4b shows the TGA diagram for as-synthesized CdO/chitosan NPs. The TG curve demonstrated a single stage of weight loss or decomposition. The temperature of about  $50\text{ }^\circ\text{C}$  represented the onset of the decomposition of CdO/chitosan NPs, which can be related to the decomposition of intermolecular bonds between chitosan structures and CdO NPs. At the temperature of about  $120\text{ }^\circ\text{C}$  the decomposition reaction was terminated or completed, and it is anticipated that the vaporization, sublimation, decomposition, oxidation, and reduction probably happened.

### 3.2. Toxicity of CdO/chitosan NPs to macrophages

To evaluate the toxicity and cytotoxic effects of CdO/chitosan NPs and amphotericin B NPs the flow cytometry analysis was used in this study. The concentration of the CdO/Chitosan core shell nanostructures that prevented the growth of 50% of the macrophages was  $1.256\text{ }\mu\text{g}/\text{mL}$ . The international selec-

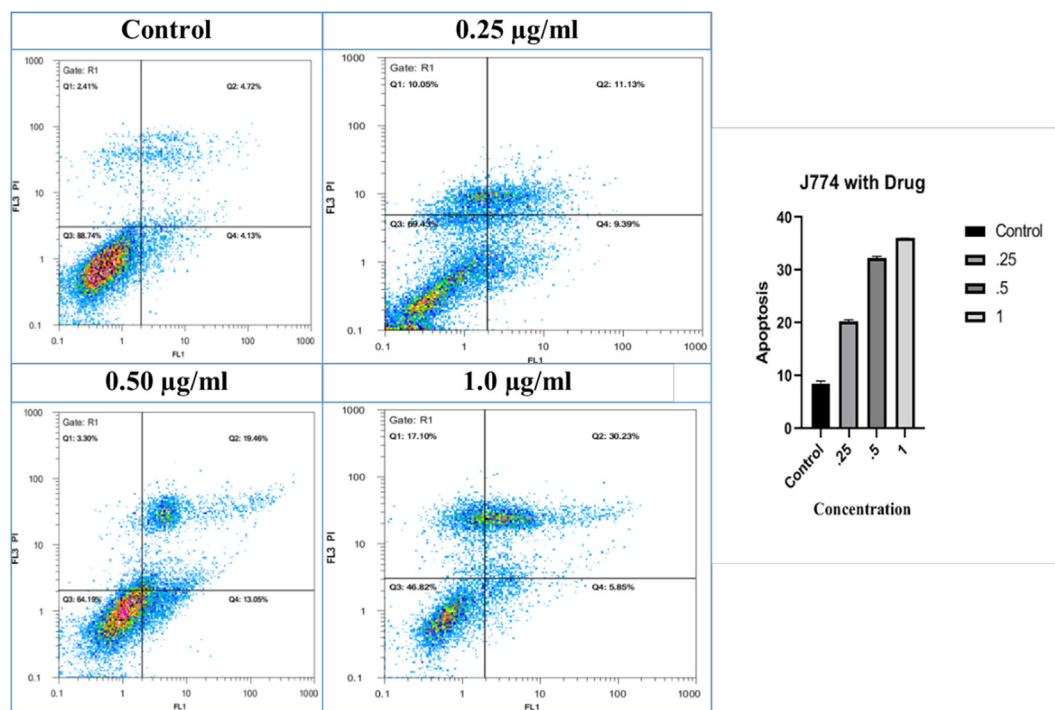


**Fig. 5** The percentage of the apoptosis macrophages at different concentrations of the CdO/Chitosan NPs such as  $0.25\text{ }\mu\text{g}/\text{ml}$ ,  $0.5\text{ }\mu\text{g}/\text{ml}$  and  $1\text{ }\mu\text{g}/\text{ml}$  with control sample (Mean  $\pm$  SD,  $n = 2$ ).

**Table 2** Toxicity of CdO/Chitosan NPs on macrophages and the lethal effect on *Leishmania major* promastigotes.

Compound	IC <sub>50</sub> Promastigotes (µg/ml)	CC <sub>50</sub> Macrophages (µg/ ml)	SI
chitosan/cadmium oxide	0/6	1/256	2.09

tivity index (SI) in Eq. (1) was estimated at about 2.09 for nanostructures. Therefore, it can be concluded that CdO/chitosan NPs have low toxicity to macrophages. Fig. 5 shows the percentage of the apoptotic macrophages at different concentrations of CdO/chitosan NPs such as 0.25 µg/mL, 0.5 µg/

mL, and 1 µg/mL with the control sample (mean±SD, n = 2). The SI for CdO/chitosan NPs is estimated in Table 2.

SI (selectivity index) =  $\frac{CC_{50} \text{ (macrophages)}}{IC_{50} \text{ (promastigotes)}}$  ≥ 1, not toxic (Neira et al., 2019) (1)

Fig. 6a and b shows the percentage of apoptosis of *Leishmania major* at different concentrations of 0.25 µg/mL, 0.5 µg/mL, and 1 µg/mL with the control sample (mean ± SD, n = 2) of CdO/Chitosan core shell nanostructures and amphotericin B, respectively. The results indicated that due to the exposure of the parasites to nanostructures, promastigotes were killed by programmed cell death. The percentage of programmed cell death was increased with respect to drug concentrations; although, these levels were lower than when the parasites were exposed to amphotericin B, so that at

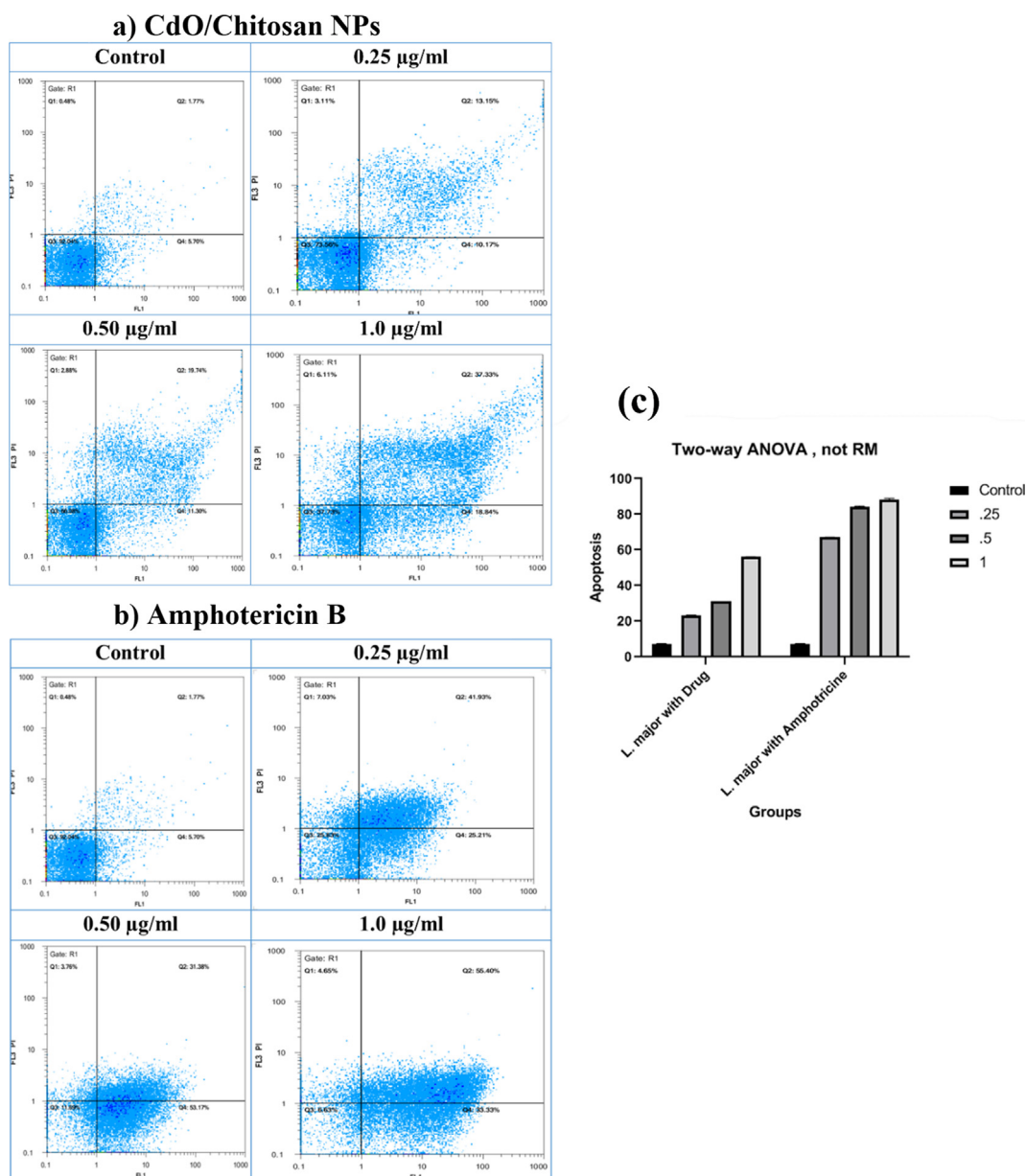


**Fig. 6** The percentage of the apoptosis of *Leishmania major* in different concentrations such as 0.25 µg/ml, 0.5 µg/ml and 1 µg/ml with control sample (Mean ± SD, n = 2) of (a) CdO/Chitosan NPs and (b) amphotericin B.

**Table 3** The effect of different concentrations of the CdO/Chitosan NPs on the number of macrophages repeated twice.

Concentration $\mu\text{g/ml}$	CdO/Chitosan core shell nanostructures	
	Mean $\pm$ SD	<i>p</i> -Value
Negative control	8.425 $\pm$ 0.181	<i>p</i> < 0.0001
0.25	20.26 $\pm$ 0.068	<i>p</i> < 0.0001
0.5	32.26 $\pm$ 0.068	<i>p</i> < 0.0001
1	36.04 $\pm$ 0.002	<i>p</i> < 0.0001

the concentrations of 0.25  $\mu\text{g/mL}$ , 0.5  $\mu\text{g/mL}$ , and 1  $\mu\text{g/mL}$ , the percentage of apoptosis was equal to 23%, 30%, and 56%. According to this study, the rate of control apoptosis was 8% and the rate of apoptosis caused by amphotericin B in similar concentrations was about 67%, 84%, and 88%, respectively.

Table 3 presents the effect of different concentrations of CdO/chitosan NPs on the number of macrophages (repeated twice). As shown by the results, by increasing the concentration of CdO/chitosan NPs from negative control up to 0.25  $\mu\text{g/mL}$ , 0.5  $\mu\text{g/mL}$ , and 1  $\mu\text{g/mL}$ , the number of macrophages significantly increased (mean  $\pm$  SD) (*p*-value

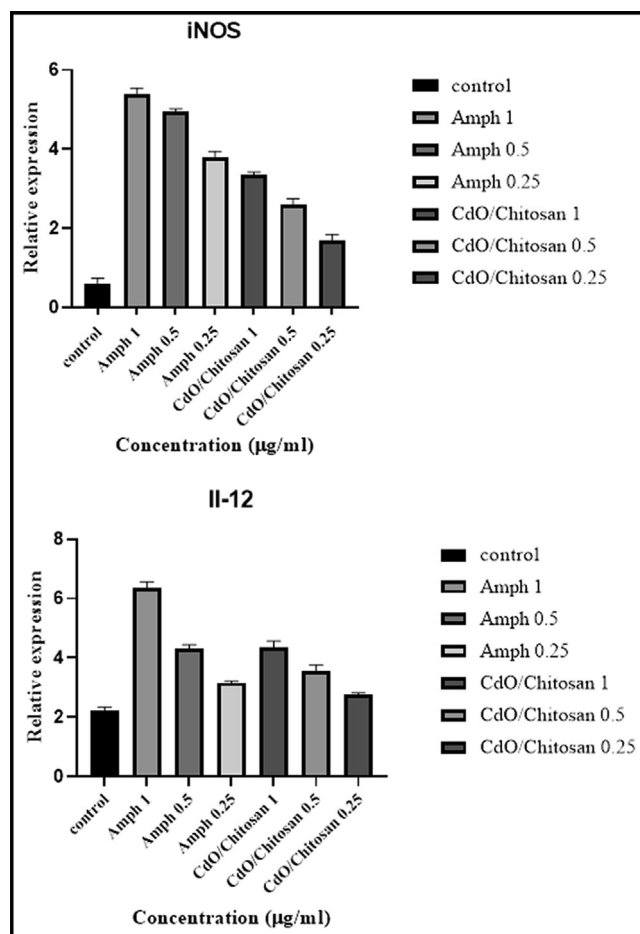


**Fig. 7** The gene expression levels of interleukin-12 (IL-12 p40) and inducible nitric oxide synthase (iNOS gene) as representative of the Th-1 pathway significantly up-regulated ( $P < 0.001$ ).

**Table 4** The effect of different concentrations of CdO/Chitosan NPs and Amphotericin B on the number of promastigotes.

Concentration $\mu\text{g/ml}$	Mean $\pm$ SD, <i>p</i> < 0.0001	
	Amphotericin B	Chitosan/CdO
Negative control	7.235 $\pm$ 0.055	7.235 $\pm$ 0.055
0.25	67.07 $\pm$ 0.005	23.16 $\pm$ 0.026
0.5	84.275 $\pm$ 0.076	31.02 $\pm$ 0.0004
1	88.365 $\pm$ 0.133	56.085 $\pm$ 0.007

< 0.0001). Considering that resistance to drugs in cutaneous leishmaniasis is increasing and due to the toxicity of these drugs, the results of the present study showed that CdO/chitosan NPs reduce the number of promastigotes. This function can be due to the direct effect of the drug on promastigotes, the immunomodulatory properties, inducing the expression of stimulatory genes such as metacaspase, inducible nitric oxide synthase (*iNOS*), interleukin-12 (*IL-12*), interferon gamma (*IFN- $\gamma$* ), tumor necrosis factor- $\alpha$  (*TNF- $\alpha$* ), and inhibiting the expression of the *IL-10* gene. Table 4 presents the effect of different concentrations of CdO/chitosan NPs and amphotericin B on the number of promastigotes. The aim of this study was to evaluate the effect of different concentrations of CdO/chitosan NPs compared with the selected and common drug (amphotericin B) on the survival and activity of *Leishmania major* promastigotes using flow cytometry.

### 3.3. Gene expression

The gene expression levels of IL-12 p40 and iNOS, as the representative of the Th1 pathway, were significantly up-regulated ( $P < 0.001$ ) with the increase of drug concentrations from 0.25  $\mu\text{g/mL}$  to 1  $\mu\text{g/mL}$  (Fig. 7). In this study, it was investigated that whether CdO/chitosan NPs mediate iNOS and cytokines induction in *L. major* parasites as a possible mode of action contributing to cell death. Treatments with CdO/chitosan NPs for 72 h greatly increased IL-12 and iNOS gene expression. Considering that resistance to the drugs used for treating cutaneous leishmaniasis is increasing and due to the toxicity of these drugs, the results of this study revealed that chitosan/cadmium oxide NPs reduce the number of promastigotes. This function is due to the direct effect of the drug on promastigotes and also through the immunomodulatory property and inducing the expression of stimulatory genes such as iNOS and IL-12.

## 4. Conclusion

In this study, two different methods (DLS and SEM) were used to determine the size and distribution of CdO/Chitosan core shell nanostructures. The green synthesis of nanoparticles is one of the most effective and least expensive methods of making nanoparticles (Zhao et al., 2021) which used in this study. These nanostructures can be used as therapeutic drugs in various treatments such as antibacterial, antifungal, antiviral, biofilm eradication, and cancer treatments. According to the findings, it can be concluded that CdO/chitosan NPs

caused the apoptosis of promastigotes of the *Leishmania major* parasites. One of the limitations of using anti-leishmaniasis drugs is their high toxicity. Studies performed to identify effective and safe anti-leishmaniasis drugs have proven that there is a strong correlation between the results of in vitro mammalian cell toxicity and the results of in vivo toxicity; the toxicity evaluated as the SI parameter higher than one shows the specificity of the proposed NPs on the parasite and its non-toxicity to macrophages.

### Declaration of Competing Interest

The authors declare that they have no known competing financial interests or personal relationships that could have appeared to influence the work reported in this paper.

### Acknowledgments

Authors are grateful to council of Pharmaceutics Research Center, Institute of Neuropharmacology, Kerman University of Medical Sciences, Kerman, Iran. This study is related to the research dissertation of Mr. Sina Bahraminegad.

### Compliance with ethics requirements

This article does not contain any studies with human subjects.

### References

- Aderibigbe, B.A., 2017. Metal-based nanoparticles for the treatment of infectious diseases. *Molecules* 22 (8), 1370.
- Akbari, M., Oryan, A., Hatam, G., 2017. Application of nanotechnology in treatment of leishmaniasis: a review. *Acta Trop.* 172, 86–90.
- Alrajhi, A., 2003. Cutaneous leishmaniasis of the old world. *Skin Therapy Lett.* 8 (2), 1.
- Arvizo, R.R. et al, 2012. Intrinsic therapeutic applications of noble metal nanoparticles: past, present and future. *Chem. Soc. Rev.* 41 (7), 2943–2970.
- Belani, H. et al, 2012. Integrated prevention services for HIV infection, viral hepatitis, sexually transmitted diseases, and tuberculosis for persons who use drugs illicitly: summary guidance from CDC and the US Department of Health and Human Services. *Morbidity and Mortality Weekly Report: Recommendations and Reports* 61 (5), 1–43.
- Boeckx, B., Maes, G., 2012. The conformational behavior and H-bond structure of asparagine: A theoretical and experimental matrix-isolation FT-IR study. *Biophys. Chem.* 165, 62–73.
- Carvalho, S.H. et al, 2019. American tegumentary leishmaniasis in Brazil: a critical review of the current therapeutic approach with systemic meglumine antimoniate and short-term possibilities for an alternative treatment. *Trop. Med. Int. Health* 24 (4), 380–391.
- Casa, D. et al, 2018. Bovine serum albumin nanoparticles containing amphotericin B were effective in treating murine cutaneous leishmaniasis and reduced the drug toxicity. *Exp. Parasitol.* 192, 12–18.
- Cortie, M.B., McDonagh, A.M., 2011. Synthesis and optical properties of hybrid and alloy plasmonic nanoparticles. *Chem. Rev.* 111 (6), 3713–3735.
- Croft, S., Olliaro, P., 2011. Leishmaniasis chemotherapy—challenges and opportunities. *Clin. Microbiol. Infect.* 17 (10), 1478–1483.
- Edrisiyan, G., 1996. Visceral Leishmaniasis in Iran and the role of serological tests in the diagnosis and epidemiological studies. *J. Kerman Univ. Med. Sci.* 3 (2), 97–108.
- Engelbrekt, C. et al, 2009. Green synthesis of gold nanoparticles with starch–glucose and application in bioelectrochemistry. *J. Mater. Chem.* 19 (42), 7839–7847.
- Fanti, J.R. et al, 2018. Biogenic silver nanoparticles inducing *Leishmania amazonensis* promastigote and amastigote death in vitro. *Acta Trop.* 178, 46–54.
- Foroughi, M.M., Pardakhty, A., Ranjbar, M., 2017. Simple microwave synthesis of CdO/Clay nanocomposites and investigation its application for degradation of MB. *J. Cluster Sci.* 28 (3), 1685–1692.
- Ghorbani, M., Farhoudi, R., 2018. Leishmaniasis in humans: drug or vaccine therapy?. *Drug Design Dev. Therapy* 12, 25.
- Gopinath, V. et al, 2016. In vitro toxicity, apoptosis and antimicrobial effects of phyto-mediated copper oxide nanoparticles. *RSC Adv.* 6 (112), 110986–110995.
- Hussain, I. et al, 2016. Green synthesis of nanoparticles and its potential application. *Biotechnol. Lett.* 38 (4), 545–560.
- Kassiri, H., Feizhaddad, M.-H., Abdehpanah, M., 2014. Morbidity, surveillance and epidemiology of scorpion sting, cutaneous leishmaniasis and pediculosis capitis in Bandar-mahshahr County, Southwestern Iran. *J. Acute Dis.* 3 (3), 194–200.
- Khanjani, N. et al, 2018. *Vaccines for preventing cutaneous leishmaniasis*. *Cochrane Database System. Rev.* 2018 (1).
- Khatami, M. et al, 2018. Core@ shell nanoparticles: greener synthesis using natural plant products. *Appl. Sci.* 8 (3), 411.
- Kubba, R. et al, 1987. Clinical diagnosis of cutaneous leishmaniasis (oriental sore). *J. Am. Acad. Dermatol.* 16 (6), 1183–1189.
- Liu, J. et al, 2006. Facile “green” synthesis, characterization, and catalytic function of  $\beta$ -D-glucose-stabilized Au nanocrystals. *Chem. – Eur. J.* 12 (8), 2131–2138.
- López-Lorente, A., Simonet, B., Valcárcel, M., 2011. Analytical potential of hybrid nanoparticles. *Anal. Bio Chem.* 399, 43–54.
- Ma, D.-D., Yang, W.-X., 2016. Engineered nanoparticles induce cell apoptosis: potential for cancer therapy. *Oncotarget* 7 (26), 40882.
- Moemenbellah-Fard, M. et al, 2003. The PCR-based detection of *Leishmania major* infections in *Meriones libycus* (Rodentia: Muridae) from southern Iran. *Ann. Trop. Med. Parasitol.* 97 (8), 811–816.
- Neira, L.F., Mantilla, J.C., Escobar, P., 2019. Anti-leishmanial activity of a topical miltefosine gel in experimental models of New World cutaneous leishmaniasis. *J. Antimicrob. Chemother.* 74 (6), 1634–1641.
- Ng, L.Y. et al, 2013. Polymeric membranes incorporated with metal/metal oxide nanoparticles: a comprehensive review. *Desalination* 308, 15–33.
- Ong, Z.Y. et al, 2017. Multibranched gold nanoparticles with intrinsic LAT-1 targeting capabilities for selective photothermal therapy of breast cancer. *ACS Appl. Mater. Interfaces* 9 (45), 39259–39270.
- Parizi, M.H., et al., 2019. Antileishmanial activity of niosomal combination forms of tiroxolone along with Benzoxonium Chloride against *Leishmania tropica* 57(4), p. 359.
- Parveen, K., Banse, V., Ledwani, L., 2016. Green synthesis of nanoparticles: their advantages and disadvantages. *AIP Conference Proceedings*. AIP Publishing LLC.
- Premanathan, M. et al, 2011. Selective toxicity of ZnO nanoparticles toward Gram-positive bacteria and cancer cells by apoptosis through lipid peroxidation. *Nanomed. Nanotechnol. Biol. Med.* 7 (2), 184–192.
- Raveendran, P., Fu, J., Wallen, S.L., 2003. Completely “green” synthesis and stabilization of metal nanoparticles. *J. Am. Chem. Soc.* 125 (46), 13940–13941.

- Shen, J. et al, 2014. Recent development of sandwich assay based on the nanobiotechnologies for proteins, nucleic acids, small molecules, and ions. *Chem. Rev.* 114 (15), 7631–7677.
- Tabrizi, M.A., Varkani, J.N., 2014. Green synthesis of reduced graphene oxide decorated with gold nanoparticles and its glucose sensing application. *Sens. Actuators, B* 202, 475–482.
- Tan, W., Donovan, M.J., Jiang, J., 2013. Aptamers from cell-based selection for bioanalytical applications. *Chem. Rev.* 113 (4), 2842–2862.
- Tiuman, T.S. et al, 2011. Recent advances in leishmaniasis treatment. *Int. J. Infect. Dis.* 15 (8), e525–e532.
- Zain, N.M., Stapley, A., Shama, G., 2014. Green synthesis of silver and copper nanoparticles using ascorbic acid and chitosan for antimicrobial applications. *Carbohydr. Polym.* 112, 195–202.
- Zhao, X. et al, 2008. Preparation of silica-magnetite nanoparticle mixed hemimicelle sorbents for extraction of several typical phenolic compounds from environmental water samples. *J. Chromatogr. A* 1188 (2), 140–147.
- Zhao, H. et al, 2021. Gram-scale synthesis of carbon quantum dots with a large Stokes shift for the fabrication of eco-friendly and high-efficiency luminescent solar concentrators. *Energy Environ. Sci.*
- Zink, A.R. et al, 2006. Leishmaniasis in ancient Egypt and upper Nubia. *Emerg. Infect. Dis.* 12 (10), 1616.